Int. J. of Thermal & Environmental Engineering
Volume 3, No. 2 (2011) 67-72

An Optimal Two-Dimensional Geometry of Flywheel for Kinetic Energy Storage

Mofid Mahdi *

Department of Mechanical Engineering, King Faisal University, Al-Ahsa, 31982, Saudi Arabia

Abstract

The consumption of energy is increasing drastically. The available resources of energy are limited therefore; the search of new sources is a vital issue. This has to be done with efficient energy consumption and saving. A flywheel may provide a mechanical storage of kinetic energy. A capable flywheel must have a very high rotational speed which may lead to a high stresses. The stress state relies on the flywheel material properties, geometry and rotational speed. On the other hand, the stored kinetic energy relies on the mass moment of inertia and rotational speed. This paper considered three solid flywheel disk profiles that are constructed using functions of cubic splines. Using FEM, the cubic splines parameters are analyzed systematically to seek a maximum stored kinetic energy per unite mass. Subjected to maximum permissible effective stress, favorable flywheel disk profiles were achieved. All FEM computations were carried out using ANSYS.

Keywords: *Flywheel Profile , Energy Storage, FEM, Stresses, Cubic Splines.*

1. Introduction

Flywheels are used to achieve smooth operation of machines. Their mechanical model of consists of a solid wheel attached to an axle. On the other hand, flywheels are constructed to store mechanical energy that may be transferred to and from an integrated motor/generator. Thus flywheels can be used as supplementary energy storage for a wide range of applications including electric vehicles, intermediate storage for renewable energy generation. One of the key issues for viable flywheel construction is its robustness and overall efficiency. Robustness of a flywheel is related to the induced stress due to high centrifugal forces generated by rotational speed. A flywheel efficiency includes the amount of specific kinetic energy (energy per unit mass) and mechanical losses. To achieve a reliable performance of a flywheel the maximum specific kinetic energy should be accomplished subjected to the maximum allowable induced stresses. The stresses of flywheels may be determined by analytical and/or numerical methods. Gerard C. Pardoen et al [1] analyzed the variation of the mass and stiffness properties of thick rim flywheel in a search for desirable stress states. To optimize the flywheel geometry, Nadar D. Ebrahimi [2] devised a continuous function for thickness variation of the flywheel calculated its volume and mass moment of inertia and presented the stress analysis problem as a two-point, boundary-value differential equation. The objective function was the ratio of inertia over volume. Kress [3] considered finding the best thickness distribution along the radius of a centrally bored flywheel under the objective of reaching an even stress distribution. A two-dimensional Finite-Element-Method (FEM) model was employed for shape optimization. Eraslan [4] used Tresca's yield criterion to investigate the elastic–plastic deformation of a rotating solid disk of exponentially varying thickness. Based on Tresca's yield criterion, Eraslan [5] obtained analytical solutions for the elastic–plastic stress distribution in rotating variable thickness annular disks subjected to plane stress assumption. The thickness of the disk is assumed to vary in parabolic form in radial direction. Arslan [6] studied flywheel profiles characterized by straight/concave or convex shaped 2D cross-sections and ranked them according to their energy storage performance. FEM was used by employing ANSYS.

Using FEM through ANSYS package, this paper discussed the details of optimization of 2D flywheel profiles characterized by set of cubic splines functions.

2. Problem Model

2.1. Flywheel Geometry

Flywheel geometry consists of solid disk as shown in Fig. 1. The flywheel is a solid disk with a constant angular velocity, ω rotating around z direction. The problem domain is represented by r, θ and z coordinates. As the disk thickness and therefore

* Corresponding author. Tel.: +96635895402
Fax: +96635817068; E-mail: mmahdi@kfu.edu.sa

DOI: 10.5383/ijtee.03.02.002

the developed centrifugal forces distribution are not affected by θ, the problem becomes axisymmetric. Therefore the solution domain can be reduced to r and z coordinates. Thus the model is simplified as 2D. The disk is symmetric across z direction and the problem can be further simplified by considering positive z direction only as illustrated by Figure 2.

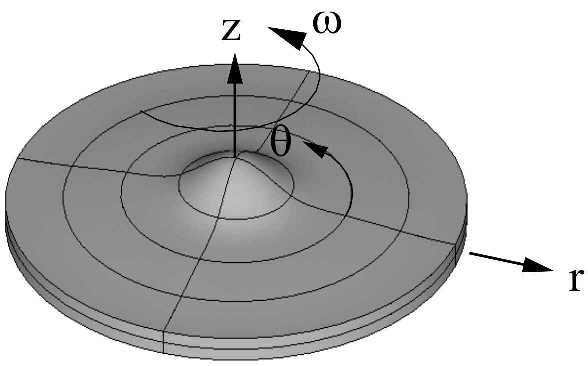

Fig. 1. Typical flywheel disk geometry

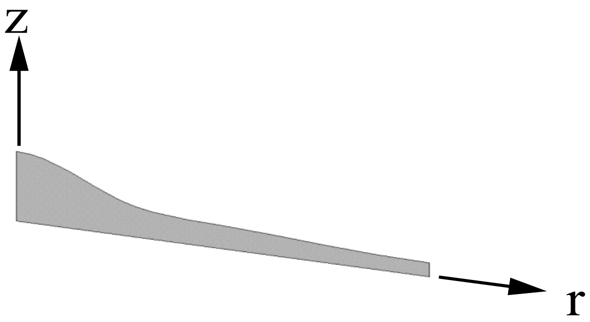

Fig. 2. Typical 2D flywheel disk profile

ANSYS is employed to determine the stress state, mass moment of inertia and stored kinetic energy of a flywheel. Accurate representation of solution domain should be fulfilled as different geometry profiles of flywheel will be utilized for optimization process. To meet this, the option of smart finite element mesh is activated by ANSYS. A finer FEM mesh is used for a thinner disk. Axisymmetric elements of 8 nodes are utilized throughout this study. Figure 3 illustrates a typical FEM mesh with symmetric boundary conditions applied at z=0.

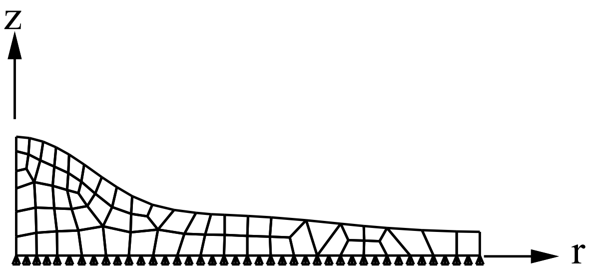

Fig. 3. Typical 2D FEM mesh of flywheel disk profile

For the sake of analysis three geometry cases were analyzed. For case 1, the thickness of flywheel is modeled by a single cubic spline function which has zero and infinite slopes at r=0 and $r=r_o$ respectively where r_o is the outer radius of flywheel. The thickness of flywheel at r=zero equals w. The geometry of case 1 is shown in Figure 4. It has three key-points needed for ANSYS mesh generation.

Case 2 has a profile with a single cubic spline function and four key-points as in Fig. 5. The cubic spline function has two slopes of zero values.

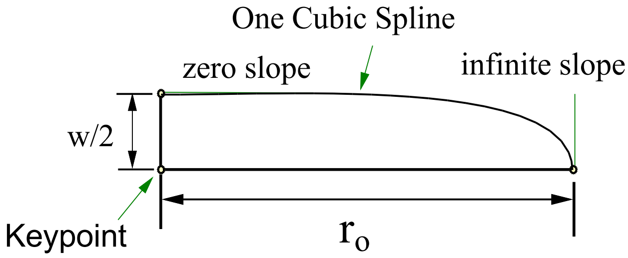

Fig. 4. Case 1 of flywheel thickness profile

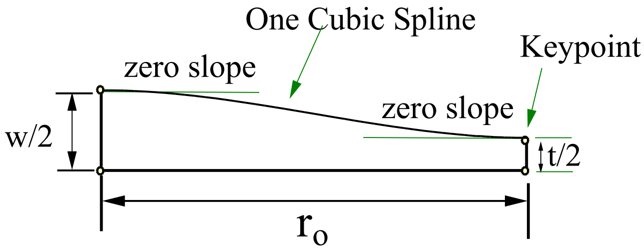

Fig. 5. Case 2 of flywheel thickness profile

The thickness of flywheel at $r=r_o$ is denoted by t.
Case 3 has similar number of key-points as those of case 2 but with an additional cubic spline. The thickness t is at intermediate distance r= r* that separates the two cubic splines. Case 3 has combined shapes as those of case 1 and 2 as demonstrated by Fig. 6.

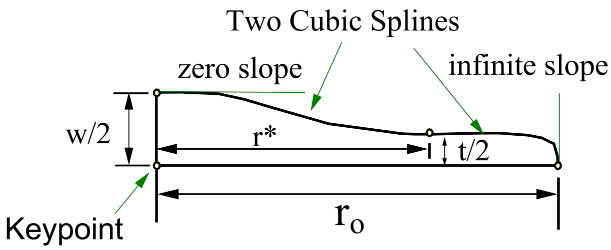

Fig. 6. Case 3 of flywheel thickness profile

2.2. Flywheel Energy

The flywheel material has 205 GPa stiffness, 290 MPa yield stress, 0.29 Poisson's ratio and a density of 7872 kg/m^3. The flywheel material is linear elastic.
The stored kinetic energy of a flywheel, KE, is

$$KE = \frac{1}{2} I \omega^2 \tag{1}$$

where I is the mass moment of inertia and ω is the angular velocity. The kinetic energy per unit mass of a flywheel (energy storing capability of flywheel), KE/m is

$$KE / m = \frac{I \omega^2}{2 \rho \int_v dv} \tag{2}$$

where v is volume, ρ is the density of flywheel material.

The mass of flywheel used is 10 kg for all cases. To achieve this, firstly a full 3D volume is generated from arbitrary sized 2D profile of flywheel, secondly the volume is re-adjusted such that the total mass becomes 10 kg. The mass moment of inertia of this volume is thereafter calculated. Finally the original 2D profile is regenerated with the new scale. All the above steps are done by APDL language of ANSYS that is written through text file. Each case study has one text (batch) file that is recalled by ANSYS.

3. Results and Discussion

3.1. Accuracy

To gain reliable numerical solution, the FEM results should be compared with associated analytical ones. To achieve this, a thin rotating disk of unit radius is considered. Hence, the plane stress condition is assumed. Both hoop ($\sigma_{\theta\theta}$) and radial stresses (σ_{rr}) were investigated. The analytical stresses solutions of a rotating thin disk are [7]

$$\sigma_{\theta\theta} = \rho\omega^2 \left(\frac{3+\nu}{8}\right)\left(r_o^2 - \frac{1+3\nu}{3+\nu} r^2\right) \quad (3)$$

$$\sigma_{rr} = \rho\omega^2 \left(\frac{3+\nu}{8}\right)\left(r_o^2 - r^2\right) \quad (4)$$

where υ is Poisson's ratio. A typical comparison of radial stresses for analytical against FEM solution is illustrated via Figs. 7.

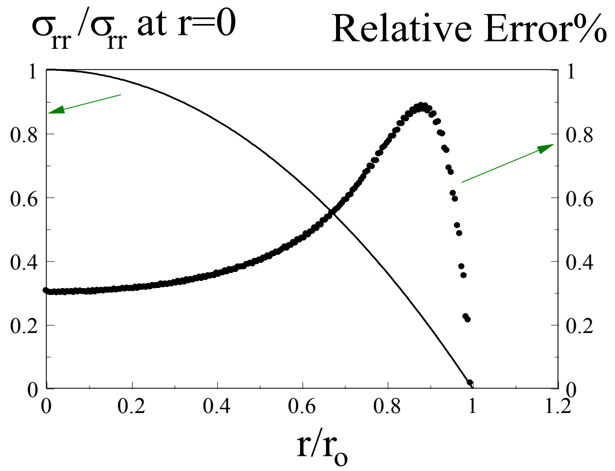

Fig. 7. Typical analytical solution and accuracy of radial stress distribution for a thin rotating disk

Figure 7 shows that the maximum relative error is less than 1% and is located near r/r_o = 0.9. The relative errors at r=zero is 0.3%. This indicates that the FEM solution of flywheel stress is in very good agreements with associated analytical plane stress results.

3.2. Results and Discussion

This study is concerned with finding an optimal flywheel stored kinetic energy with the restriction of elastic deformation. Therefore, the maximum von Misses (effective) stress (σ_e) should not exceed the yield stress (σ_y) of flywheel material (i.e 290 MPa). The examination of Eq. 3 and 4 shows that the maximum effective stress should be proportional to ω^2 such that

$$\sigma_e = c\omega^2 \quad (5)$$

where c is constant that relies on the shape of flywheel and can be obtained from FEM analysis using a fixed magnitude of ω. This study uses ω = 1000 rad/sec. The maximum permissible rotational speed, ω_{max} , therefore, is

$$\omega_{\max} = 1000 \times \sqrt{\frac{290MPa}{\sigma_e}} \quad (6)$$

Eq. 6 eliminates the need of defining a state variable while performing design optimization. By recalling Eq. 2 and adjusting mass of flywheel as 10 kg, the allowable KE/m_a is therefore

$$KE / m_a = \frac{I\omega_{\max}^2}{20} \quad (7)$$

Consequently the remaining task is reduced to become a maximization of KE/m_a or minimization of $1/(KE/m_a)$.

The subsequent results are demonstrating the variation of KE/m_a with flywheel profile parameters. Fig. 8 illustrates the optimization analysis of Case 1. Here, there is one parameter of optimization (i.e. w/r_o). A thinner disk (with a lower w/r_o) has a higher mass moment of inertia, I and vice versa. A higher mass moment of inertia, I, leads to a higher stresses therefore a lower permissible rotational speed, ω_{max}, should be employed. Eq. 1 shows that capability of flywheel is proportional to both flywheel mass moment of inertia and rotational speed. Therefore intermediate magnitudes of I and ω are anticipated to yield optimal conditions. This study indicates that there is an optimal shape of flywheel at w/r_o =0.56.

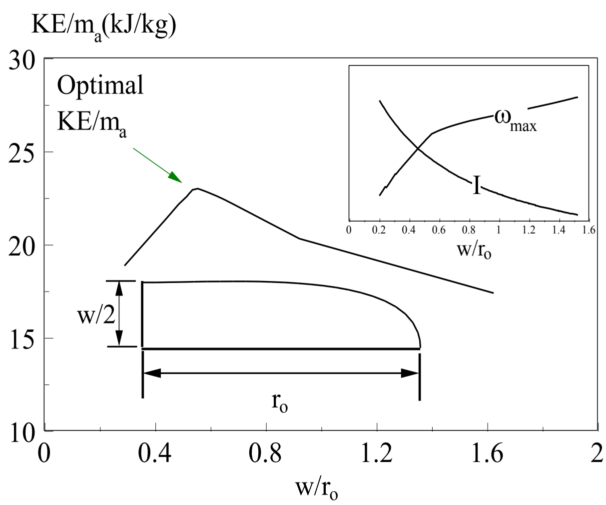

Fig. 8 Optimization analysis of case 1

A flywheel with Case 2 has two optimization parameters, namely, w/r_o and t/w ratios. Fig. 9 shows the plot of the influence of t/w ratio at different w/r_o magnitudes.

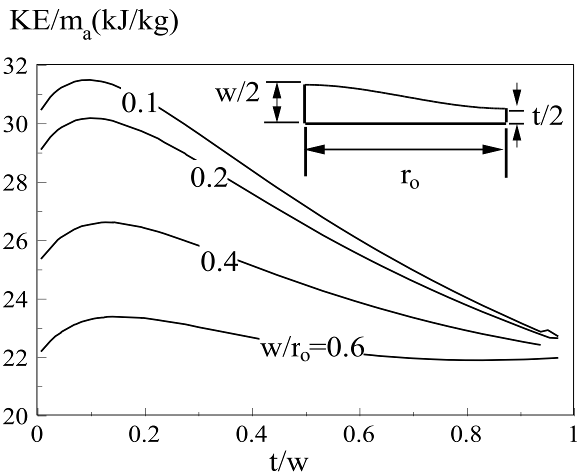

Fig. 9 Optimization analysis of case 2, the role of thickness ratio, t/w

For a given w/r_o ratio, a larger t/w magnitude may lead to higher mass moment of inertia and therefore larger stresses which requires the reduction of rotational speed. On return, this will result in lowering KE/m_a. A very small t/w ratio, on the other hand, results into smaller mass moment of inertia, I, and thus a smaller KE/m_a. It is found that t/w of 0.12 has local optimal values of KE/m_a the magnitude of which increases as w/r_o decreases as in Fig. 10.

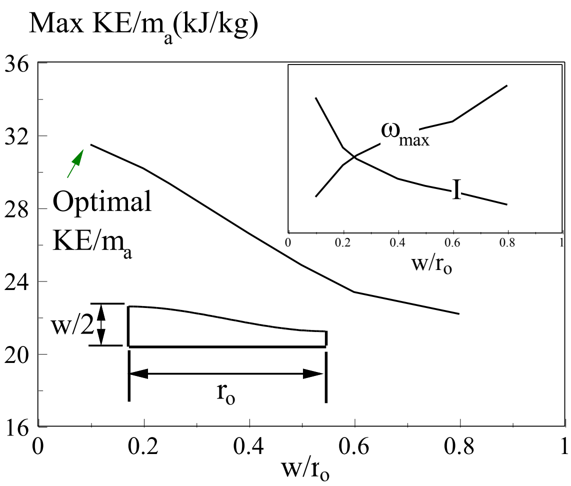

Fig. 10 Optimization analysis of case 2, the role of thickness ratio, w/r$_o$

As for case 1 a thinner disk has a higher mass moment of inertia, I, and a lower permissible rotational speed, ω_{max}. An optimal KE/m_a is obtained at w/r_o= 0.1. This analysis indicates that a very thin disk is required in order to have the highest stored KE/m_a. However, a very thin flywheel disk has a tiny robustness and very large tendency of buckling.

A flywheel of Case 3 has three parameters of geometry profiles, t/w, w/r_o and r^*/r_o ratios. The latter parameter (i.e. r^*/r_o) divides the shape of flywheel into two cubic splines functions (Recall Fig. 6). For a given thickness ratio (w/r_o =0.4), the permissible stored kinetic energy is considered in relation to t/w thickness ratio and the geometrical ratio r^*/r_o as illustrated via Fig. 11.

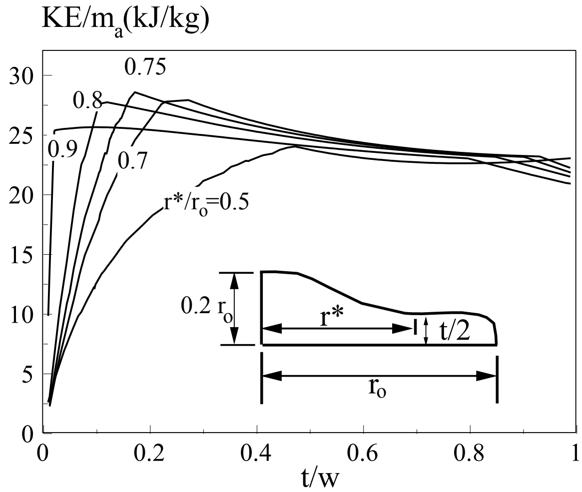

Fig. 11 Optimization analysis of case 3, the role of thickness ratio, t/w and geometry parameter r*/r$_o$ (w/ r$_o$ =0.4)

It is found that r^*/r_o ratio has noticeable effect on the permissible stored energy. A smaller and a larger r^*/r_o ratios result in smaller permissible stored kinetic energy. Thus an intermediate r^*/r_o ratio has an optimal KE/m_a. Similar observations are noticed for smaller w/r_o magnitudes (i.e. w/r_o =0.2 and w/r_o =0.1) as illustrated via Fig. 12 and Fig. 13 respectively. A flywheel with smaller thickness ratio, w/r_o, has a higher optimal permissible stored energy.

Figure 14 illustrates the maximum kinetic energy storing capability associated with thickness ratio w/r_o. As for case 2, an optimal geometry has the smallest thickness, which leads to the same restrictions as those applied for case 2.

Fig 15 illustrates the shapes and dimensions of optimized profiles of cases. Fig. 15 shows that the shapes of flywheel for both Case 2 and Case 3 are close to each other in terms of overall dimensions. When compared with other cases, Case 1 has a thicker and shorter flywheel. Therefore, Case 2 and Case 3 are anticipated to yield close results in terms of permissible stored energy, KE/m_a.

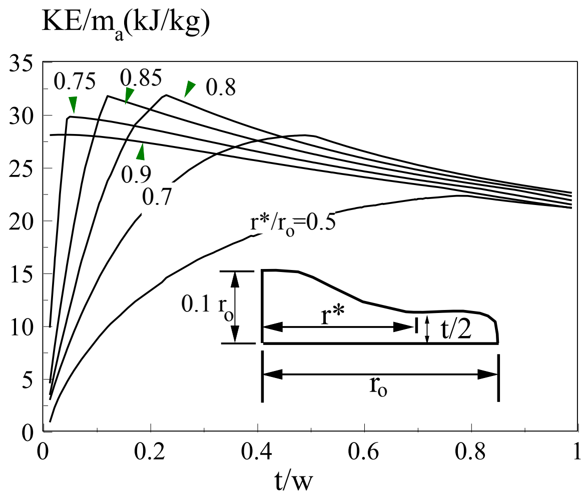

Fig. 12 Optimization analysis of case 3, the role of thickness ratio, t/w and geometry parameter r*/r$_o$ (w/ r$_o$ =0.2)

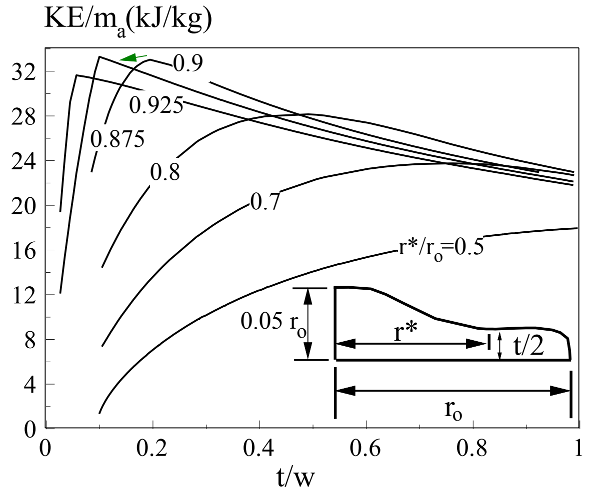

Fig. 13 **Optimization analysis of case 3, the role of thickness ratio, t/w and geometry parameter r^*/r_o (w/ r_o =0.1)**

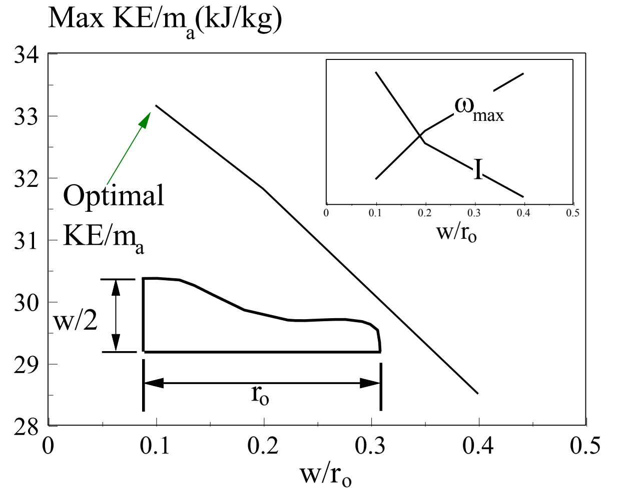

Fig. 14 **Optimization analysis of case 3, the role of thickness ratio w/ r_o**

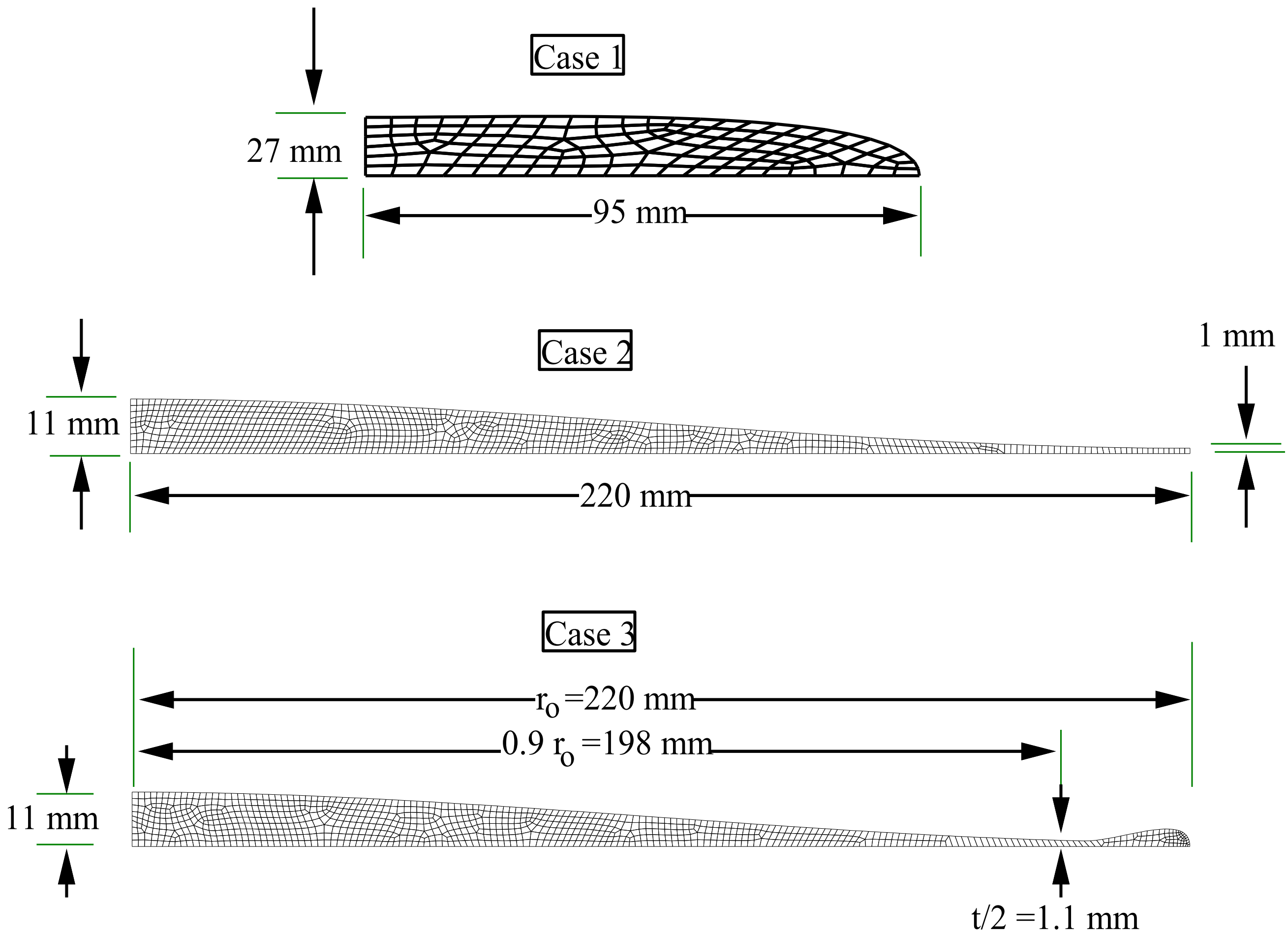

Fig. 15 **Optimized cases shapes**

To investigate the stress state of each case under maximum permissible stored energy, Fig 16 is considered. It is found that for all cases the maximum effective stress is near r=0. The effective stresses are decreasing as r is increasing. Therefore the flywheel thickness at r =0 has to be maximum. Case 3 has the maximum capability of kinetic energy storing at lower rotational flywheel speed. Case 2 has less capability with slightly higher rotational speed. Case 1 has the highest rotational speed and the lowest capability of kinetic energy storing.

4. Conclusion

Using FEM, this paper investigated near optimal shapes of flywheels for kinetic energy storing. Three flywheels thickness profiles were analyzed based on cubic splines functions. The study concluded that: (1) A more cases of flywheel disk thickness functions should be analyzed, (2) a thinner flywheel disk has a higher capability of kinetic energy storing, and (3) the corresponding maximum effective stresses are found near the centre of flywheels where thickness should maximum.

Acknowledgments

This optimization analysis is based ANSYS FEM. The author wishes to thank The College of Engineering at King Faisal University-KSA for all supports provided.

References

[1] Gerard C. Pardoen, Rod D. Nudenberg and Bruce E. Swartout, Achieving desirable stress states in thick rim rotating disks, International Journal of Mechanical Sciences 1981; 23/ 6; 367-382. http.dx.doi.org/10.1016/0020-7403(81)90066-7

[2] Nadar D. Ebrahimi, Optimum design of flywheels, Computers and Structures 1988;29/ 4; 681-686. http.dx.doi.org/10.1016/0045-7949(88)90379-3

[3] G.R. Kress, Shape optimization of a flywheel, Structural and Multidisciplinary Optimization 2000;19/1;74-81. http.dx.doi.org/10.1007/s001580050087

[4] A.N. Eraslan, Y. Orcan, Elastic–plastic deformation of a rotating solid disk of exponentially varying thickness, Mechanics of Materials 2002; 34; 423–432. http.dx.doi.org/10.1016/S0167-6636(02)00117-5

[5] Ahmet N. Eraslan, Elastic–plastic deformations of rotating variable thickness annular disks with free, pressurized and radially constrained boundary conditions, International Journal of Mechanical Sciences 2003;45; 643–667. http.dx.doi.org/10.1016/S0020-7403(03)00112-7

[6] Mehmet Ali Arslan, Flywheel geometry design for improved energy storage using finite element analysis, Materials and Design 2008; 29; 514–518. http.dx.doi.org/10.1016/j.matdes.2007.01.020

[7] Shigley JE: Mechanical engineering design. McGraw-Hill, 1977.

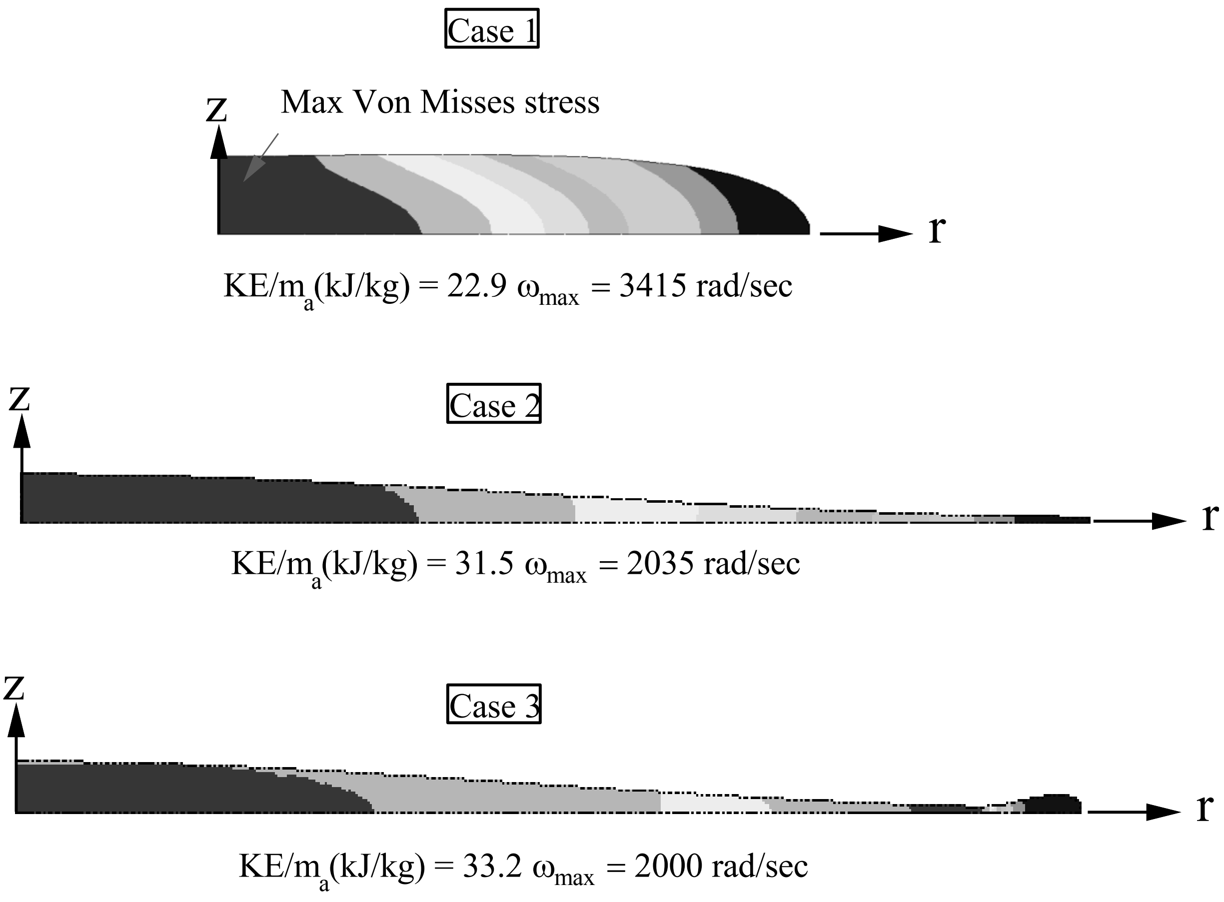

Fig. 16 Capability and Stress State of Flywheel Optimized Cases